

Observed Performance of Long Steel H-Piles Jacked into Sandy Soils

J. Yang, M.ASCE¹; L. G. Tham, M.ASCE²; P. K. K. Lee³; and F. Yu⁴

Abstract: Full-scale field tests were performed to study the behavior of two steel H-piles jacked into dense sandy soils. The maximum embedded length of the test piles was over 40 m and the maximum jacking force used was in excess of 7,000 kN. The test piles were heavily instrumented with strain gauges along their shafts to measure the load transfer mechanisms during jacking and the subsequent period of static load tests. Piezometers were installed in the vicinity of the piles to monitor the pore pressure responses at different depths. The time effect and the effect of installation of adjacent piles were also investigated in this study. The test results indicated that, although both piles were founded on stiff sandy strata, most of the pile capacity was carried by shaft resistance rather than base resistance. This observation implies that the design concept that piles in dense sandy soils have very large base capacity and small shaft resistance is likely to be inappropriate for jacked piles. It was also found that the variation in pore pressures induced by pile jacking was closely associated with the progress of pile penetration; the pore pressure measured by each piezometer reached a maximum when the pile tip arrived at the piezometer level. A nearby pile jacking was able to produce large tensile stresses dominating in the major portion of an installed pile; both the magnitude and distribution of the induced stresses were related to the penetration depth of the installing pile.

DOI: 10.1061/(ASCE)1090-0241(2006)132:1(24)

CE Database subject headings: Field tests; Interactions; Piles; Pore pressures; Sand.

Introduction

Jack piling is a pile installation technique that involves the use of hydraulic jacks to press piles into the ground. Compared to conventional dynamic piling methods, such as vibrators and drop hammers, jack piling has some attractive advantages. First, the process is essentially free from noise and vibration and is hence a particularly suitable method for installing piles in noise and/or vibration-sensitive areas. Second, the load capacity of each pile can be assured, as the jacking procedure essentially proof-tests the pile to near ultimate capacity during installation.

In early days, jacked piles were mainly used to underpin existing foundations to increase capacity and reduce settlement. Nowadays, they are increasingly used as foundations for new structures. The behavior of jacked piles therefore becomes of primary concern in these applications. However, there is a scarcity of field data on the performance of jacked piles. In some field studies on the behavior of driven piles (Cooke et al. 1979; Konrad

and Roy 1987; Bond and Jardine 1991; Lehane et al. 1993; Chow 1995), jacking instead of dynamic driving was used to install test piles to prevent damage to instruments on the piles. These studies inadvertently provided useful information on the mechanisms involved with jacked piles.

The field tests conducted by Lehane et al. (1993) and Chow (1995), in particular, dealt with piles in sand. Lehane et al. (1993) investigated the shaft resistance of a steel pile jacked into a loose to medium-dense sand deposit. Chow (1995) reported test data on the stress interactions between two adjacent piles jacked in a dense sand deposit. In both studies, the piles had conical tips and their diameters and lengths were 102 mm and 6 m, respectively, (i.e., Imperial College model piles). The maximum jacking forces applied were 97 and 275 kN, respectively. In practical applications, the jacking force required to press long piles into dense sand deposits may be significantly larger than such values. To the writers' best knowledge, there is very little data on the behavior of long piles with large capacity/jacking load in dense sandy soils.

As an alternative to full-scale tests, well-designed laboratory experiments in the centrifuge or chamber (e.g., De Nicola and Randolph 1997; Lehane and Gavin 2001) may play a role in understanding the performance of jacked piles in sandy soil. It is, however, widely recognized that small-scale model tests include unavoidable limitations in capturing the field behavior of piles in sandy soil (Craig and Sabagh 1994; Fellenius 2002; Yang 2005). The behavior of sand and/or sandy soil is complicated and depends on many factors, including two important ones: relative density and stress level (Been and Jefferies 1985; Bolton 1986; Yang and Li 2004). This state dependency, together with the difficulty of modeling the real pile-soil interaction process in the laboratory, suggests that carefully designed field tests with highly instrumented piles provide the key to understanding the mechanisms that govern pile behavior.

It is against this background that a comprehensive field study

¹Assistant Professor, Dept. of Civil Engineering, The Univ. of Hong Kong, Pokfulam, Hong Kong, China. E-mail: junyang@hku.hk

²Professor, Dept. of Civil Engineering, The Univ. of Hong Kong, Pokfulam, Hong Kong, China.

³Head, Dept. of Civil Engineering, The Univ. of Hong Kong, Pokfulam, Hong Kong, China.

⁴Research Student, Dept. of Civil Engineering, The Univ. of Hong Kong, Pokfulam, Hong Kong, China.

Note. Discussion open until June 1, 2006. Separate discussions must be submitted for individual papers. To extend the closing date by one month, a written request must be filed with the ASCE Managing Editor. The manuscript for this paper was submitted for review and possible publication on April 12, 2004; approved on December 17, 2004. This paper is part of the *Journal of Geotechnical and Geoenvironmental Engineering*, Vol. 132, No. 1, January 1, 2006. ©ASCE, ISSN 1090-0241/2006/1-24-35/\$25.00.

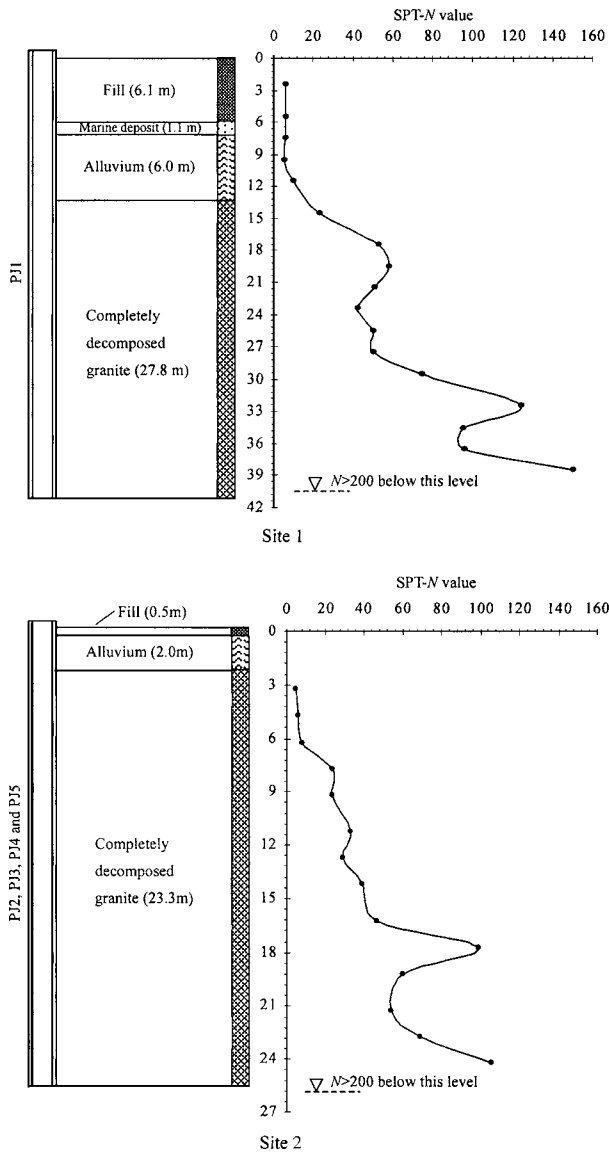


Fig. 1. Soil profiles at Sites 1 and 2

was launched to monitor piles when jacked and load tested in sandy soils. The main objectives of the study were to investigate (1) the behavior of the piles during jacking; (2) the load transfer and load settlement mechanisms of the piles; (3) the buildup and dissipation of pore pressure due to jacking; and (4) the effect of jacking on adjacent piles. All test piles involved in the study were steel H-piles. The maximum embedment depth of the piles was over 40 m, and the maximum design capacity of the piles was 3,540 kN. As the piles were jacked into stiff bearing strata, the maximum jacking force used in the tests was in excess of 7,000 kN. This is probably the highest jacking force ever used in the field.

Table 1. Details of Test Piles

Pile number	Size (kg/m)	Design capacity (kN)	Embedded length (m)	SPT-N value at pile tip	Location
PJ1	305 × 305 × 223	3,540	40.9	200	Site 1
PJ2	305 × 305 × 180	2,950	25.8	186	Site 2

This paper focuses on two test piles carried out at two sandy soil sites. Both piles were densely instrumented with strain gauges along their shafts to measure the load transfer mechanisms. Vibrating piezometers were installed in the vicinity of the piles to monitor the variation of pore pressure induced by pile jacking. The performance of the piles and surrounding soils was continually monitored during the process of jacking and the subsequent period of loading tests. Test data have been interpreted carefully and are presented in detail in this paper. It is believed that these data are very useful in efforts to validate and improve the current design methods; they also enable a better assessment of the suitability of jacked piles for practical applications. Due to the paper length limits, more theoretical discussions will be presented in separate papers in the future.

Site Conditions and Test Program

Site Conditions

The ground conditions at Site 1 comprise a sequence of fill material, marine deposit, and alluvium, overlying weathered granite strata (Fig. 1). The water level is 2.81 m below ground surface. The fill layer has a thickness of about 6.1 m, comprising loose to medium-dense, fine to coarse sand with some gravel or sandy silt. The marine deposit is composed of slightly clayey, slightly silty, fine to medium sand, and its thickness is generally small. The alluvial deposit consists of interbedding layers of clay, silt, and sand. The average thickness of the alluvial layer is about 6.0 m. The weathered granite is completely decomposed for a depth of over 20 m below the alluvial deposit. Highly decomposed granite may occasionally be encountered before reaching the bedrock at a depth of 28–55 m below ground surface.

The ground conditions at Site 2 are characterized by a vertical stratigraphic sequence of fill layer, alluvial layer, and completely decomposed granite. Firm strata formed by completely or highly decomposed granite with an SPT-N value exceeding 200 are at a depth of 26.08 m below ground surface. The fill layer mainly comprises silty fine to coarse sand with some gravels and occasionally cobbles. The alluvial deposit consists of silty fine to coarse sand with fine to medium gravel; its thickness ranges from 15 to 3.2 m. The ground water is at a depth of 3.65 m.

The completely decomposed granite (CDG) at both sites is a residual soil and is composed mainly of slightly clayey and silty sand. Its engineering property is hence close to silty sand (Lumb 1962, 1965; Guide 1988). Because of the varying degrees of weathering of the parent rock, the SPT-N values at both sites generally increase with depth. Both test piles were founded on the firm decomposed granite strata with SPT-N values greater than 150 (Fig. 1).

Instrumentation Details

The details of the two test piles, including their size, embedded length, and design capacity, are given in Table 1. The test pile at

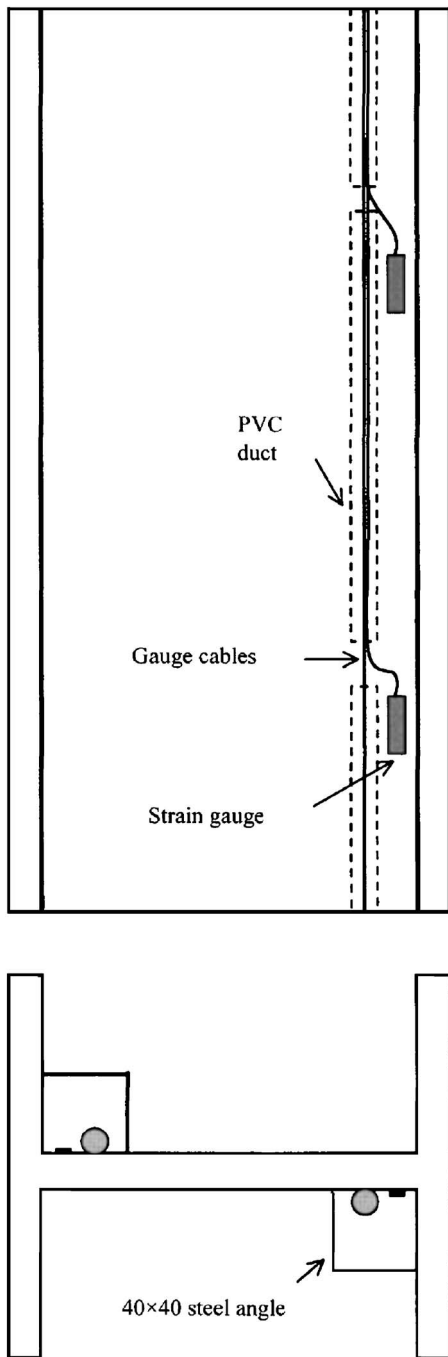


Fig. 2. Schematic arrangement for strain gauges

Site 1, denoted as PJ1, was instrumented with electrical strain gauges along its shaft, at a spacing of 3 m for the upper part and 4 m for the lower part. At each level, two strain gauges were installed at the opposite fillets of the pile. On each web side, the cables of the strain gauges were fed into a polyvinyl chloride (PVC) duct. To prevent them from damage during jacking, the strain gauges and PVC duct on each side were, further, covered by a 40×40 mm steel angle welded onto the pile. The schematic arrangement for the instruments is shown in Fig. 2.

In the vicinity of PJ1, two vibrating wire piezometers for measuring pore pressures, denoted as M1 and M2, were embedded at depths of 10 and 20 m below ground surface. The piezometers were installed inside a borehole of 100 mm diameter, the location of which was 1.75 m away from the pile center (Fig. 3). The

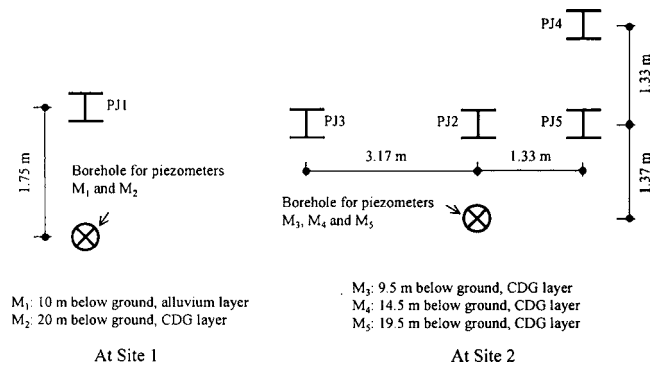


Fig. 3. Locations of piezometers for measuring pore pressure

borehole for the piezometers was filled with bentonite; at each instrument level a sand layer of 0.5–1 m was formed to ensure groundwater flow through the piezometer.

The test pile at Site 2, denoted as PJ2, was instrumented with vibrating wire strain gauges at nine sections, spaced at 2.5 m. The arrangement for the instruments was similar to that for PJ1. At a distance of 1.37 m from the center of PJ2, three piezometers, M3, M4, and M5, were installed at levels of 9.5, 14.5, and 19.5 m below the surface (Fig. 3).

Test Program

Both piles were installed by the jacking machine shown in Fig. 4. The main components of the jacking machine were clamps for holding the pile vertical and jacks for pressing the piles into the ground. The loading capacity of the machine was 9,070 kN, supplied by six hydraulic jacks. The maximum penetration per stroke was 1.8 m. The penetration rate for both piles was on the order of 1–1.8 m/min and adjusted to lower values for the last 1–2 m of penetration. Unlike dynamically driven piles, there are no well-accepted termination criteria for jacked piles due to lack of experience. The final jacking force adopted for PJ1 was about two times its working load, while for PJ2 the force was 2.3 times the working load. The final jacking force was maintained constant until pile head settlement was less than 5 mm in 15 min. The

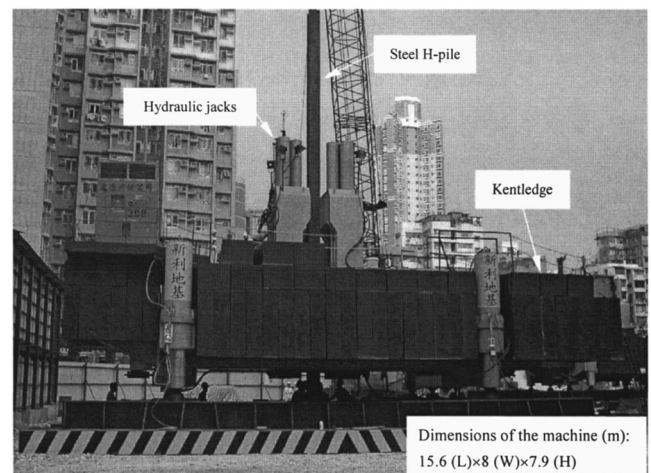


Fig. 4. Jacking machine used in tests

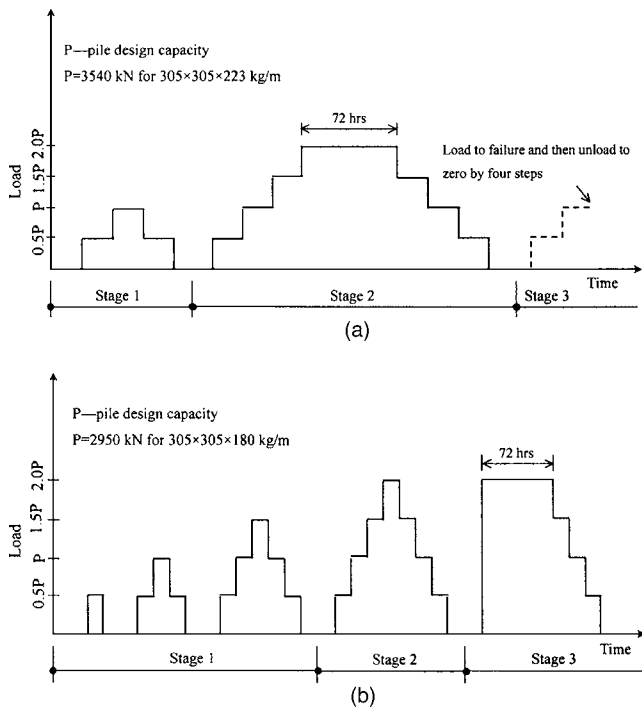


Fig. 5. Loading schemes adopted in tests: (a) PJ1; and (b) PJ2

termination criterion adopted is called “precreeping” (Li et al. 2003), which can effectively reduce the creep settlement of piles under working conditions.

The static loading test on PJ1 was carried out four days after its installation using the maintained load (ML) procedure as shown in Fig. 5(a). Pile PJ2 was load tested two days after the completion of jacking, following the loading scheme shown in Fig. 5(b). The scheme consisted of three stages: Stage 1 included three loading-unloading cycles, with a maximum load of 1.5 times the working load of the pile; Stage 2 involved loading the pile in steps to two times the working load (5,900 kN) and then unloading completely; and in Stage 3, the pile was loaded for 72 h at two times its working load and then the load was released. Note that, unlike PJ1, PJ2 was not loaded to failure in the final stage.

After the load test on PJ2, three piles adjacent to PJ2, numbered as PJ3, PJ4, and PJ5 in this paper, were jacked into the ground by the following sequence. First, PJ5, which was at a horizontal center-to-center distance of 1.33 m from PJ2 (Fig. 3), was installed. Then PJ4, at a distance of 1.33 m from PJ5, was jacked into the ground. Finally, PJ3, 3.17 m away from PJ2, was installed. All three piles had the same size as PJ2. Valuable information on the effect of adjacent pile installation was recorded.

Test Results and Discussions

Behavior of Piles during Jacking

The jacking loads during the installation of the piles were recorded and plotted as a function of penetration in Fig. 6. Clearly, for all five piles, the jacking load increased with penetration. Consequently, the induced stress in the piles also increased with increasing penetration, as shown in Fig. 7. In general, PJ1 penetrated relatively easily as compared to the other four piles; when its penetration was less than 18 m, the load was almost constant

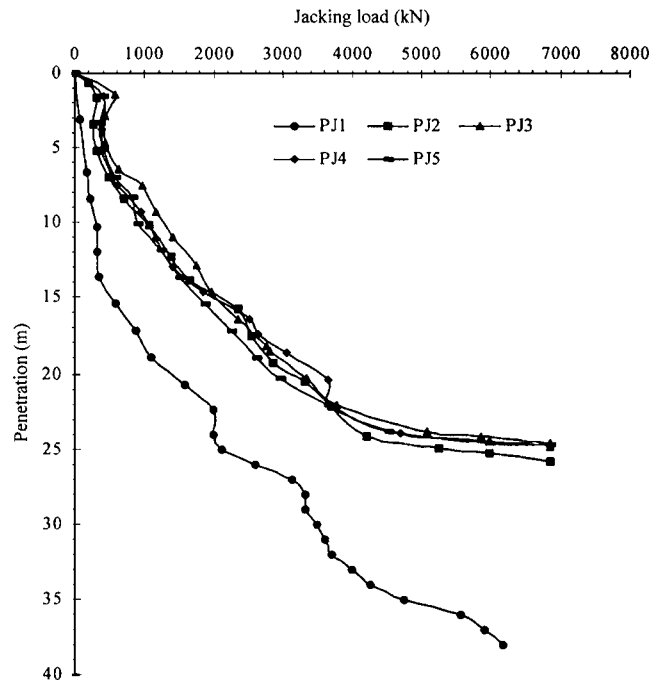


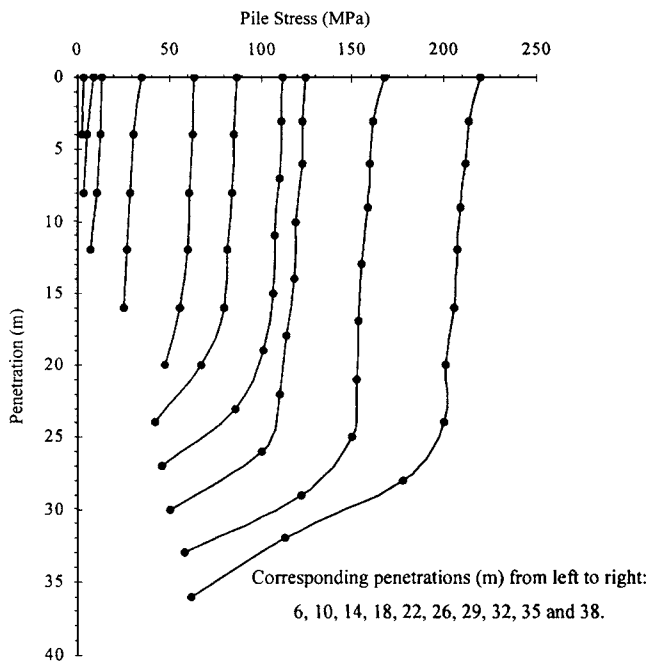
Fig. 6. Jacking force versus penetration depth

within the embedded length. Referring to the soil profile, this implies that, before the pile penetrated into the decomposed granite soil, the shaft resistance was negligible. As the pile penetrated into the decomposed granite layer, the amount of shaft resistance increased markedly.

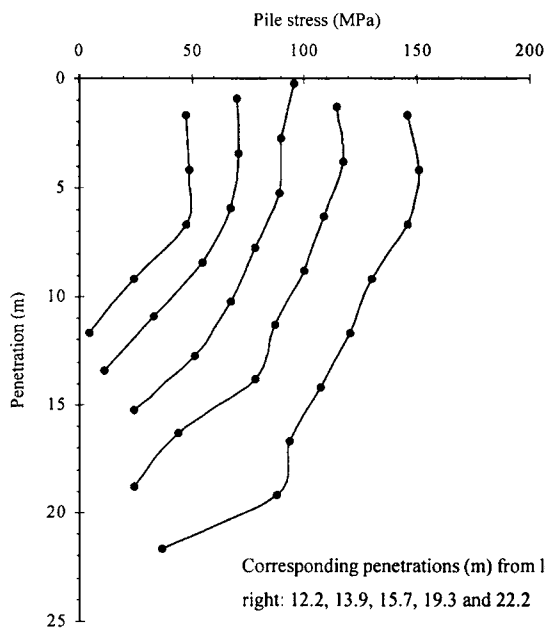
The distribution of axial load along the shaft of PJ2 during the process of jacking displayed a somewhat different feature from that of PJ1. The shaft resistance was mobilized at a relatively small penetration. For example, at a penetration of 12.2 m, the shaft friction already reached a level of about 1,300 kN, carrying more than 90% of the jacking load. For a better view of the load transfer during jacking, the shaft and base resistance are separated for both piles and shown as a function of penetration in Fig. 8.

It is now clear that for PJ1 there was a remarkable increase in both shaft and base resistance after the pile tip reached the decomposed granite layer. At a penetration of 38 m, the resistance from shaft friction was in excess of 4,000 kN, amounting to 70% of the jacking load. In comparison, both the shaft and base resistance of PJ2 increased consistently as the penetration increased. At a penetration of 22.2 m, the resistance from shaft friction reached a value of about 2,800 kN, while the resistance from end bearing was about 800 kN. The corresponding percentages of the shaft and end resistance to the applied jacking load were 78 and 22%, respectively.

The different performance observed during jacking PJ1 and PJ2 may be attributed to several reasons. One is the difference of the ground conditions at the two sites, as shown in Fig. 1. The soil profile at Site 2 is generally uniform, comprising a decomposed granite stratum extending from 2.5 m below the surface to a great depth, whereas at Site 1 there exist 13.1 m superficial deposits of fill, marine sandy soil, and alluvium whose SPT-N values are very low. The other reason is probably related to the ground loss caused by pile jacking. When an H-pile penetrates into the ground, whether by driving or jacking, the overlying soil may be dragged down by the pile to lower levels, leaving a gap between the pile and soil at upper levels. This phenomenon has been de-



(a)



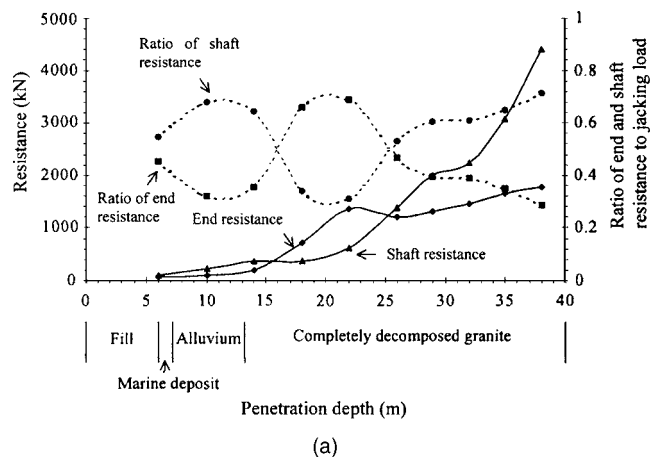
(b)

Fig. 7. Variation of axial stress during jacking: (a) PJ1; and (b) PJ2

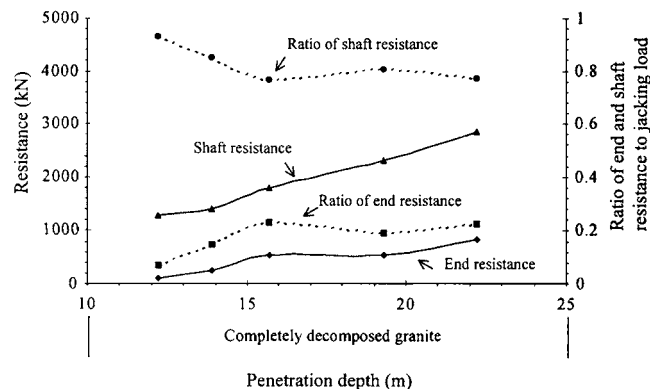
scribed by, for example, Poulos and Davis (1980). For PJ1, the generated gap was not filled until the installation was completed, whereas for piles PJ2–PJ5 the gaps were filled using sand during the process of jacking. The observed difference may be in part a reflection of the different treatments of the gaps.

Variation of Pore Pressures During Jacking

Excess pore pressures induced in surrounding soils by jacking PJ1 were recorded by piezometers M1 and M2 and are shown as a function of time in Fig. 9. The pore pressures induced by jacking PJ2 were measured by piezometers M3, M4, and M5 and shown in Fig. 10. Note that M3, M4, and M5 at Site 2 and M2 at Site 1 were all installed in the decomposed granitic soil, while M1 was



(a)



(b)

Fig. 8. Variation of end and shaft resistance during jacking: (a) PJ1; and (b) PJ2

embedded in the alluvium layer. Depending on void ratio, the permeability of decomposed granite soil may be as high as 10^{-5} m/s (Lumb 1962).

In general, the variation of pore pressures recorded by each instrument displayed a similar tendency as elaborated hereafter for M1 and M2. The pore pressure measured by M1 remained virtually unchanged from the start of jacking until the pile tip reached a depth of about 6.5 m, i.e., 3.5 m above the piezometer level. On reaching that depth, the pore pressure built up rapidly during each jacking advance and dissipated rapidly during jacking pauses. When the pile tip reached a depth of 12.5 m, i.e., 2.5 m below the instrument level, the excess pore pressure was again virtually unaffected by jacking. It is noted that the pore pressure reached a maximum when the pile tip arrived at the piezometer level.

Similarly, the measurements from M2 indicate that pile jacking had no influence on the pore pressure before the pile tip was about 6 m above the piezometer level; on reaching this depth, pore pressure built up rapidly. When the pile tip reached a depth of about 2.5 m below instrument level, the pore pressure was virtually unaffected by jacking. Again, the greatest pore pressure was measured when the pile tip reached the piezometer level.

The rapid dissipation of the excess pore pressure implies that it should not affect long-term pile behavior. Moreover, it deserves mentioning that, despite the obvious change in pore pressure during jacking, there was virtually no change in pore pressure as piles were load tested.

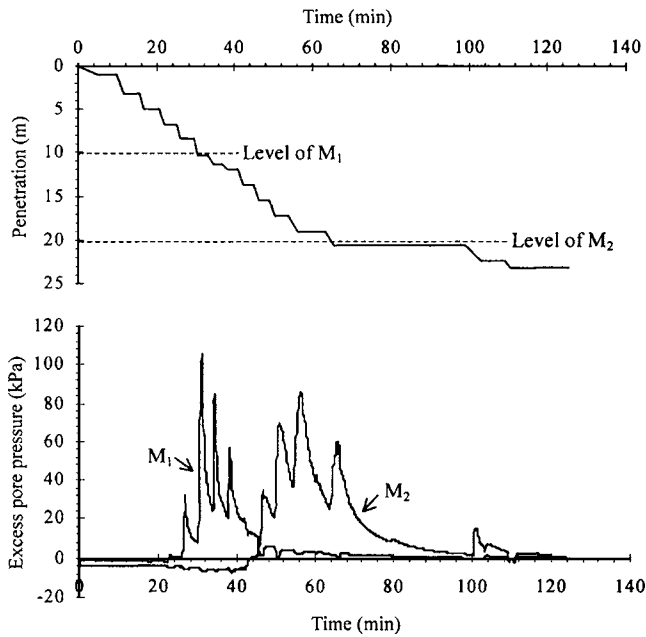
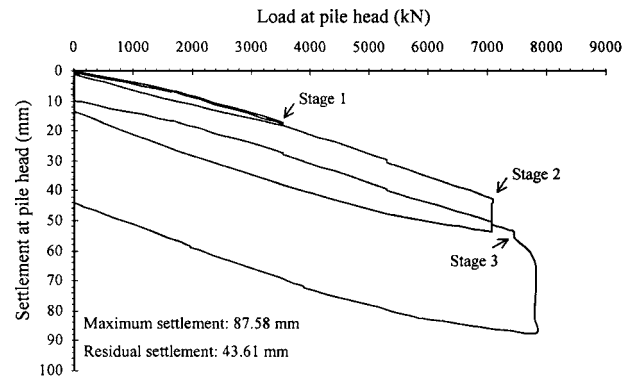


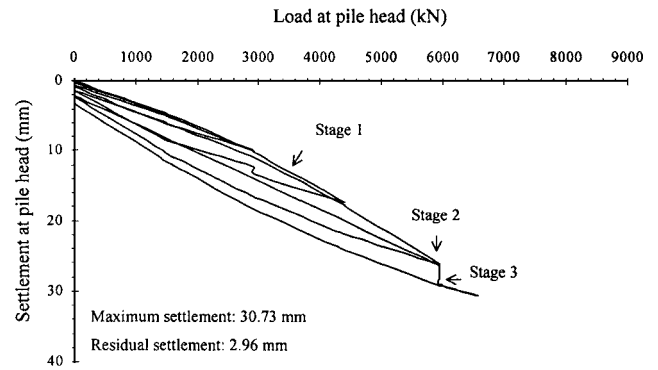
Fig. 9. Variation of pore pressures induced by jacking PJ1

Behavior of Piles during Static Load Tests

Fig. 11 shows the load-settlement curves of the two piles during loading tests. When pile PJ1 was loaded to its working load, the recorded settlement was 17.25 mm. After unloading, the residual settlement was approximately 0.75 mm. When loaded to two times the working load in the second circle, a settlement of about 42.75 mm was initially recorded. After holding the load for 72 h (as required by Hong Kong practice), the settlement increased remarkably to 53.91 mm. Clearly, the creep settlement in the 72 h period was a major contributor to the residual deformation. It is also noted that the load-settlement curve of PJ1 in Stage 2 almost



(a)



(b)

Fig. 11. Load-settlement curves: (a) PJ1; and (b) PJ2

coincided with that in Stage 1 when the load was less than the working load (3,540 kN). The pile-soil stiffness seemed not to be influenced by the loading cycle.

By comparison, PJ2 settled only 11 mm when loaded to its working load (2,950 kN) in the first cycle. In Stage 3 of the test, a settlement of 26.39 mm was recorded when the pile was loaded to two times its working load. After maintaining the load for 72 h, a small creep settlement of 2.79 mm was recorded. The residual settlement after unloading was 2.96 mm. It should be mentioned that PJ2 was once loaded to 6,600 kN for several hours in Stage 3 but it was later rectified.

Both the creep and residual settlements of PJ2 were very much reduced. The reductions were due mainly to the “precreeping” effect attained in the termination of jacking. Recall that the jacking force used in the termination stage of PJ2 was as large as 2.3 times its working load. It should also be noted that, unlike PJ1, PJ2 was not loaded to failure in the final stage.

The distributions of axial loads along the piles at various load levels are shown in Fig. 12. Note that the results for PJ1 were derived from the load test in Stage 3 and the results for PJ2 were from Stage 2 of the test. At each load level, the change in axial load in the upper part of PJ1 was insignificant, and the shaft resistance in this zone was hence very small. In the lower part of PJ1, however, substantial shaft resistance was mobilized, especially at higher load levels. In comparison, an approximately linear reduction in axial load was observed for PJ2 for all of the load levels, implying that fairly uniform shaft resistance was mobilized in the decomposed granite layer. These observations suggest that for both piles the major contribution to shaft resistance was from the decomposed granite soil.

Furthermore, it can be seen from Fig. 12 that the end bearing

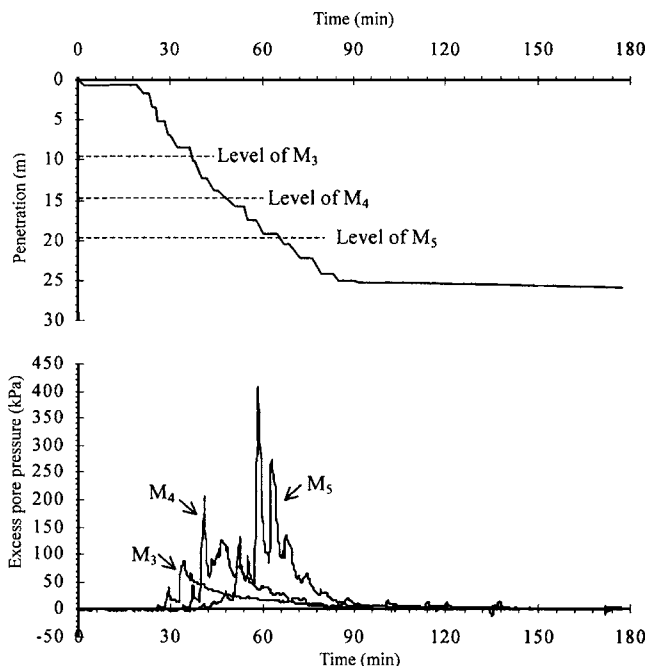


Fig. 10. Variation of pore pressures induced by jacking PJ2

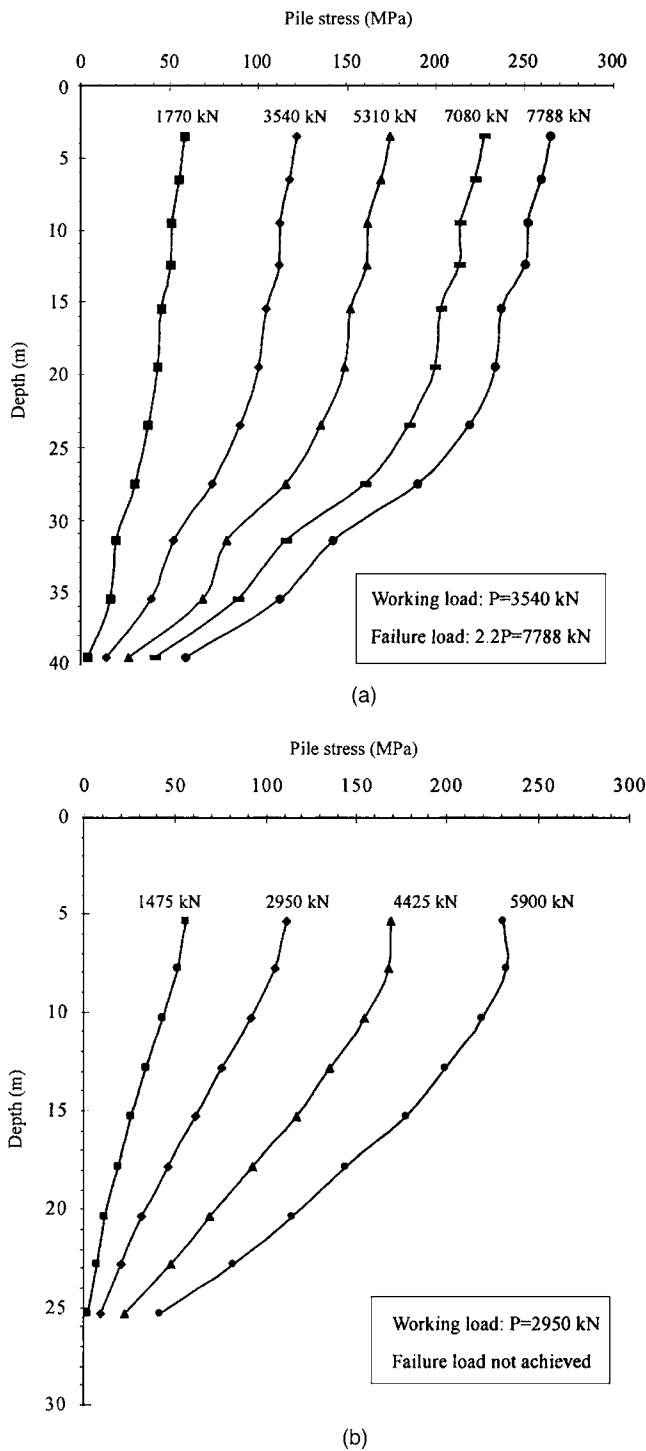


Fig. 12. Distribution of axial stress: (a) PJ1; and (b) PJ2

of both piles was increasingly mobilized as the applied load increased. To enable a better assessment, Table 2 includes key values of the base and shaft resistance at various load levels for PJ1 and PJ2, together with the values of the ratio between the end bearing and applied load. The percentage of end bearing measured for PJ1 under a half working load was 7.8%; it increased to 17.3% when the applied load was two times the working load of the pile. For the same increase in applied load, the percentage of end bearing of PJ2 increased from 11.7 to 16.9%.

The results indicate that, although both piles were founded on very firm strata, most of the applied load was carried by shaft

resistance rather than end bearing. Interestingly, it is noted that this finding is in agreement with the observations from a field test on a much shorter pile (Chow 1995). In that study, the measured ratio between the end bearing and total load was about 16.4%. Because the load transfer mechanism of piles in sand is complicated and depends on many factors, more reliable data are desired to further verify this finding.

From Fig. 12, the distributions of shaft resistance along the piles can be deduced as shown in Fig. 13. It is clear that for both piles the shaft resistance in the lower part was significantly mobilized as the applied load increased. Under the working load condition, the average shaft resistance for PJ1 and PJ2 was 41.16 and 61.63 kPa, respectively.

Shown in Fig. 14 are the shaft friction-displacement curves at various depths for both piles. Here, the so-called “local displacement” was defined as the difference between the pile head settlement and the elastic shortening of the shaft above the calculated level. Focus is turned to the completely decomposed granite, as it contributed most to shaft resistance. For PJ1, the shaft resistance was fully mobilized at a displacement of 14–16 mm, i.e., about 4% of the equivalent diameter of the pile. Note that the ultimate value of the shaft friction between depths of 35.5 and 39.5 m was up to 200 kPa. For PJ2, the shaft friction at larger depths (e.g., 22.8–25.3 m) did not show full mobilization; this was because the local displacement was too small (about 4 mm).

Time Effect

The effect of loading history on the load transfer mechanism was also recorded in the study. Fig. 15 shows the distributions of axial load along the shaft of PJ1, where the solid and dotted lines represent the distributions of axial load in Stage 1 and Stage 2, respectively. The influence of loading cycles appeared to be slight on the load distribution. A point that deserves attention is that a small amount of residual stress was locked in the pile upon unloading in Stage 1.

During the second stage of the load test on PJ1, the pile was loaded to two times its working load, and this load was maintained for 72 h. The axial stresses measured immediately after the application of the load and just before the release of the load are shown in Fig. 16. The measurements indicate that the change in either shaft or base resistance was insignificant. Similar results were reported by Hunt et al. (2002) for driven piles.

In order to further investigate the time effect on jacked piles, a second load test was conducted on PJ2, 34 days after the first test. Fig. 17 compares the load distributions derived from the two tests for the same level of applied load (5,900 kN). It was found that, after 34 days of rest, there was an increase in end bearing, from about 42.4 to 52.96 MPa. A small increase in shaft resistance in the very lower part of the pile was also measured, from 167 to 189 kPa. It is of interest to note that Chow et al. (1997) obtained a similar observation on driven piles in sand.

Effect of Installation of Adjacent Piles

As described earlier, after PJ2 was load tested, three adjacent piles, PJ5, PJ4, and PJ3 were jacked into the ground using the same jacking machine. Observations on the effect of installation of the three piles are discussed in the following.

The pore pressures measured by piezometers M3, M4, and M5 during jacking PJ5 are presented in Fig. 18. Figs. 19 and 20 show the pore pressure responses induced by jacking PJ4 and PJ3. Note

Table 2. Shaft and Base Resistance at Various Load Levels

Stage	Applied load, Q (kN)	Shaft resistance, Q_s (kN)	Base resistance, Q_b (kN)	Q_b/Q (%)
PJ1 (Stage 3)	1,770 (=0.5 P)	1,632	138	7.8
	3,540 (=1.0 P)	3,091	449	12.7
	5,310 (=1.5 P)	4,502	808	15.2
	7,080 (=2.0 P)	5,853	1,227	17.3
PJ2 (Stage 2)	1,475 (=0.5 P)	1,303	172	11.7
	2,950 (=1.0 P)	2,639	311	10.5
	4,425 (=1.5 P)	3,866	559	12.6
	5,900 (=2.0 P)	4,904	996	16.9

Note: P =design capacity of pile.

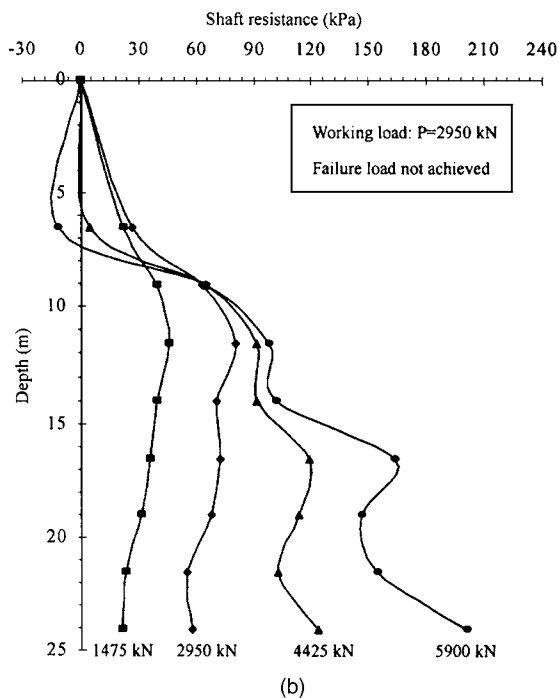
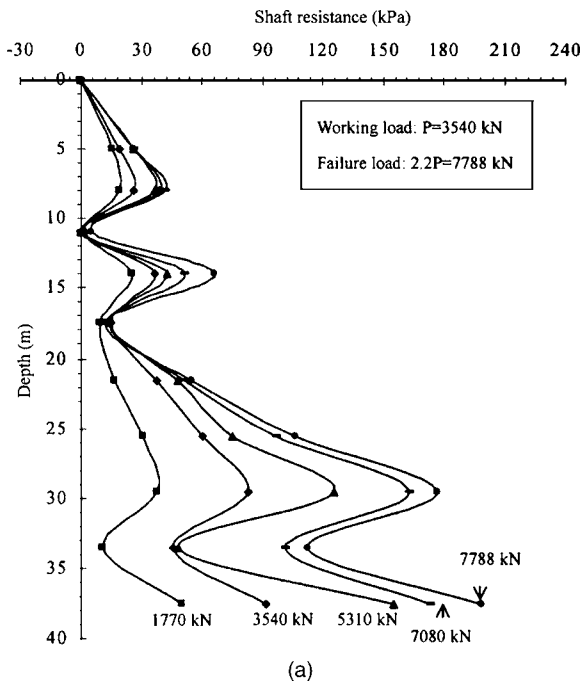


Fig. 13. Distribution of shaft resistance: (a) PJ1; and (b) PJ2

that the piezometer M3 malfunctioned during jacking PJ4 and PJ3, and its measurements are hence not included.

In general, the variation in pore pressure displayed similar features to that shown in Figs. 9 and 10. The pore pressure measured by each piezometer remained virtually unchanged before the pile tip reached a depth of about 3–4 m above the instrument level, then reached a maximum when the pile tip reached the piezometer level, and finally decreased when the pile tip passed.

By comparing the pore pressures induced by jacking PJ2, PJ3, and PJ5 (Figs. 10, 18, and 20), one may note that the magnitude of pore pressures induced by jacking PJ2 was the greatest, while that due to jacking PJ3 was the smallest. This observation is reasonable and is in good agreement with the layout of the three piles (see Fig. 3); PJ2 was closest to the piezometers and PJ3 was farthest.

A comparison of Figs. 19 and 20 however, seems to indicate

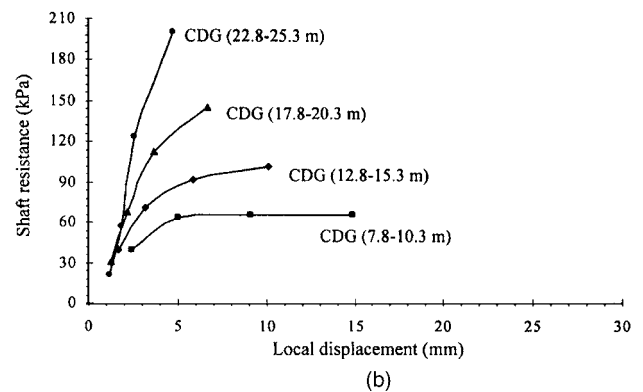
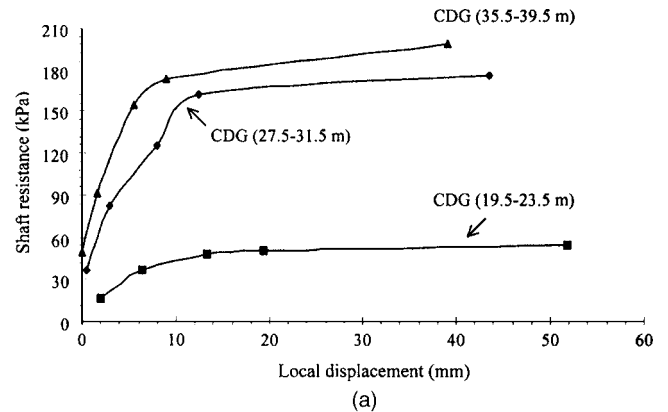


Fig. 14. Local shaft resistance versus local displacement: (a) PJ1; and (b) PJ2

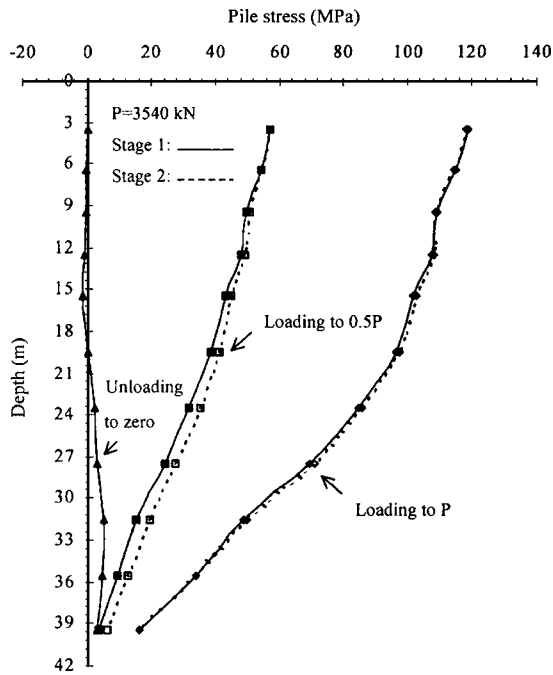


Fig. 15. Distribution of axial stress in PJ1 at different test stages

an inconsistency, if one recalls the different distances of PJ4 and PJ3 to the piezometers. This inconsistency was probably due to the screening effect from PJ2 and PJ5. Note that PJ4 was jacked after the installation of PJ2 and PJ5. Referring to Fig. 3, this implies that PJ2 and PJ5 would serve as barriers to the impact from jacking PJ4. For PJ3, however, there was no such a screening effect. As a consequence, although PJ4 was closer to the instruments than PJ3, the pore pressure measured during its installation was lower than that measured during jacking PJ3.

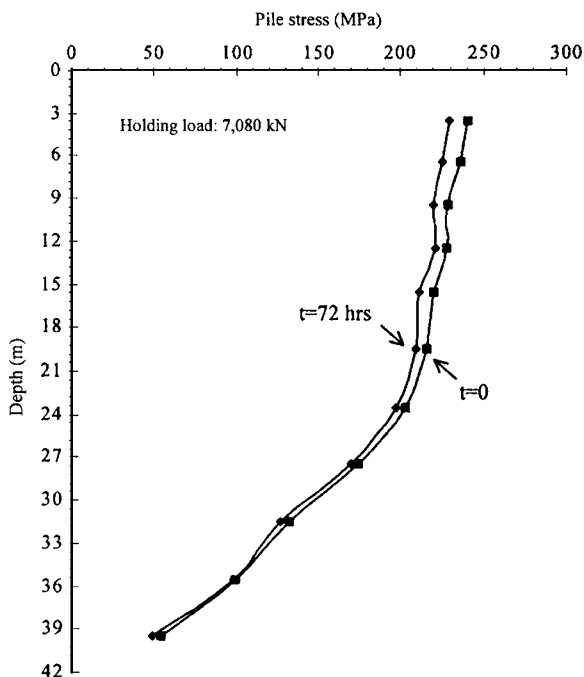


Fig. 16. Creep-related change of load distribution in PJ1

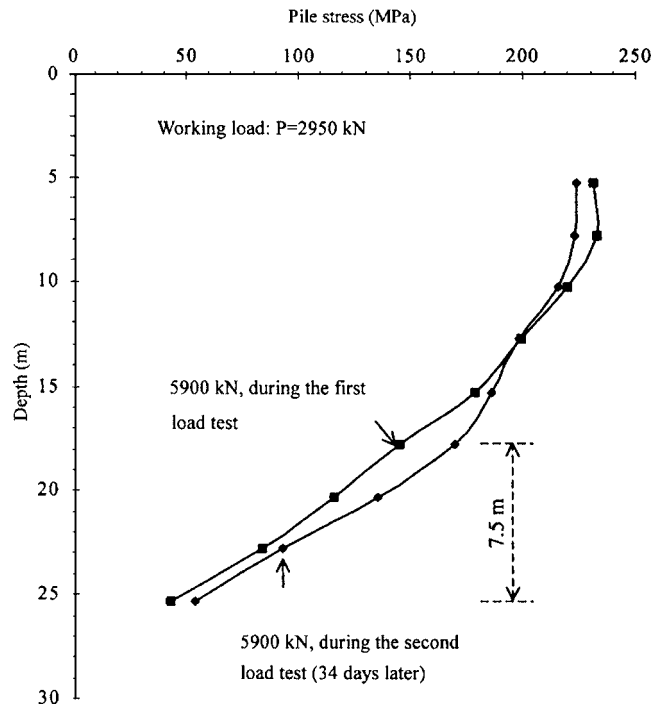


Fig. 17. Time-related change of load distribution in PJ2

The effect of pile jacking on adjacent piles is an issue of great interest. Using the test data, Fig. 21 shows the distributions of stress along the shaft of PJ2 measured during the process of jacking PJ5. Four different penetrations of PJ5, ranging from 5.15 to 24.60 m, are included.

Obviously, both the magnitude and distribution of the stress were closely associated with the penetration of PJ5. For example, when PJ5 penetrated to a level less than 5.15 m (i.e., 20% of the length of PJ2), almost no stress was induced on PJ2. At a penetration of 15.40 m (60% of the length of PJ2), significant tensile

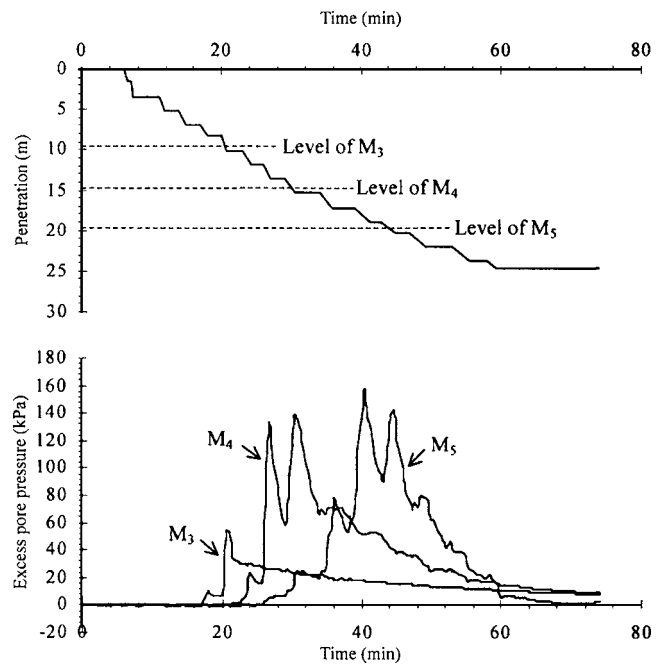


Fig. 18. Variation of pore pressures induced by jacking PJ5

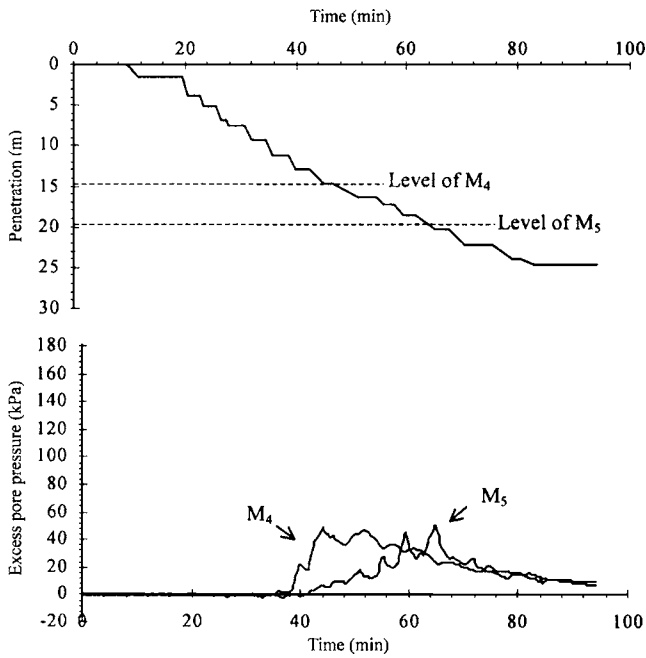


Fig. 19. Variation of pore pressures induced by jacking PJ4

stresses dominating in the major portion of the shaft of PJ2 were measured, except for the upper part, where small compressive stresses existed. At the end of installation of PJ5, the maximum tensile stress induced on PJ2 was approximately 37 MPa.

An impression from Fig. 21 is that the position of the peak tensile stress would move toward the lower part of PJ2 as the penetration of PJ5 increased and that the position was always 1–2 m below the level of the penetrating pile tip. A similar feature was observed in the numerical modeling by Poulos (1994) for the effect of pile driving on adjacent piles in clay. Qualitatively, the stress interactions observed can be attributed to the soil

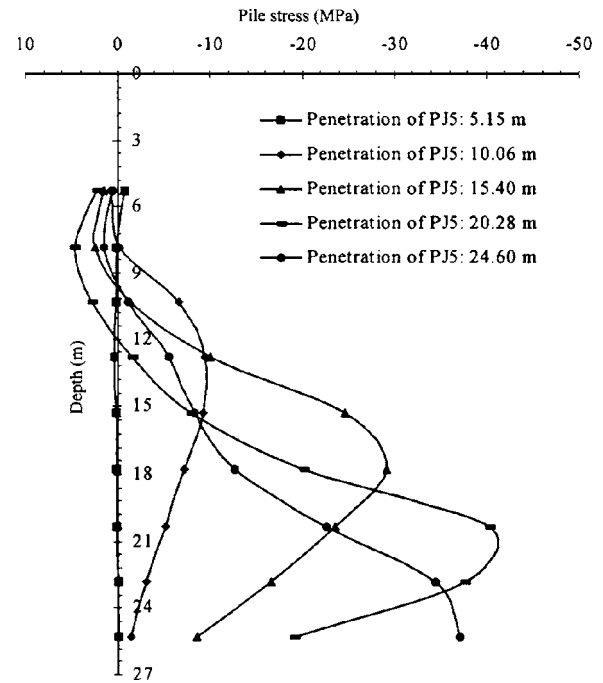


Fig. 21. Stresses in PJ2 due to jacking PJ5

movement caused by the nearby jacking; the soil movement may produce negative and positive shaft frictions in the lower and upper parts of the existing pile, respectively. To quantify the complex interaction effects involved, further research efforts are required on both experimental and theoretical aspects.

The effect of residual stress on pile response at a subsequent time is another interesting issue. A point that should be noted is that, unlike the residual stress induced by installation of the pile itself, the residual stress due to the installation of adjacent piles was mainly in tension (Fig. 21). This means the effect on pile response is generally positive. In other words, if the residual stress were not considered, the base resistance would appear

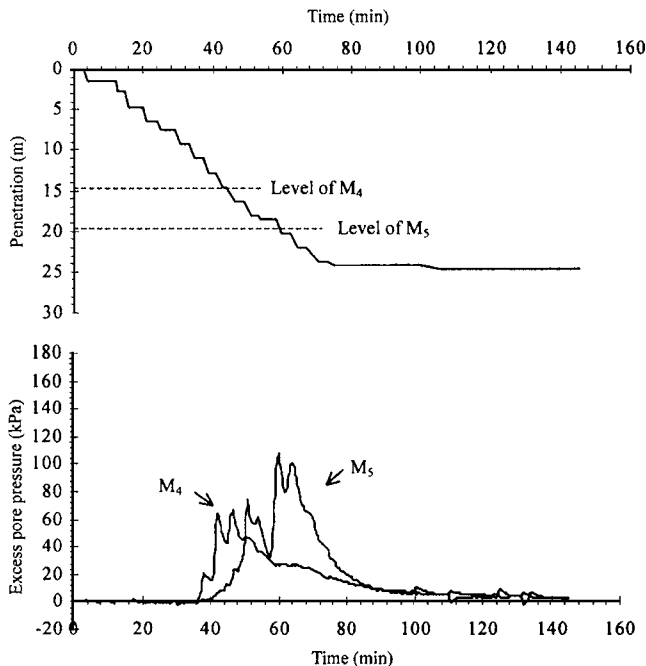


Fig. 20. Variation of pore pressures induced by jacking PJ3

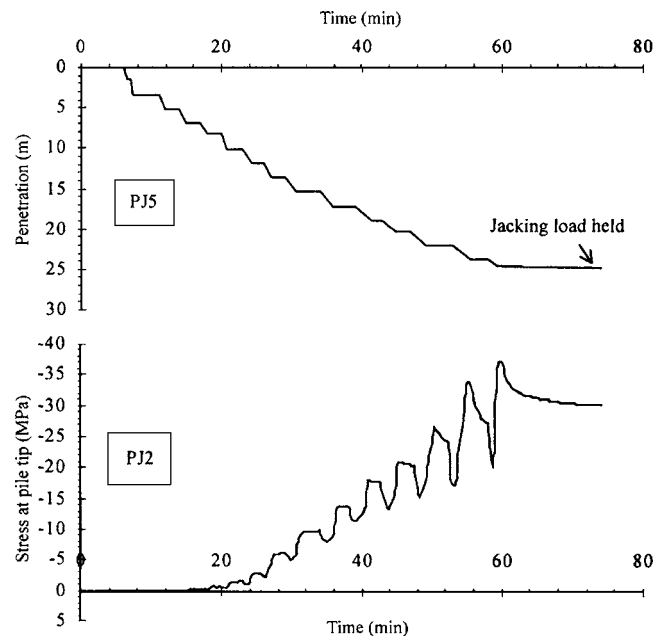


Fig. 22. Variation of stress at tip of PJ2 induced by jacking PJ5

larger than the true value, while the shaft resistance would correspondingly appear smaller than the true resistance.

Fig. 22 presents the stress measured at the tip of PJ2 during jacking PJ5. It is evident that the variation in stress was closely associated with the penetration process of PJ5 (i.e., it advances and pauses). The stress generally increased as the jacking proceeded. At the end of the installation of PJ5, the stress reached a maximum, about 30 MPa, then it started to dissipate a little when the jacking was completed.

The tensile stress at the pile tip was derived with reference to the actual H-section, whose area is very small. If converted to force, the value of 30 MPa corresponds to a magnitude of about 690 kN. If the outside cross-sectional area were used for the pile, the tensile stress calculated would reduce significantly. In a numerical analysis of the pile driving effect on adjacent piles (Poulos 1994), the maximum tensile force estimated for the existing pile (length=15 m; diameter=0.5 m) was about 300 kN. The two values are comparable, considering the fact that the test piles in this study were installed in dense granite soil while the model pile in Poulos's analysis was assumed to be embedded in a homogeneous soft clay.

A key point involved in the preceding discussion is how to choose the cross-sectional area in evaluating the end bearing of H-piles. This is a tricky issue in relation to soil plugging. For driven H-piles, there are generally two extreme cases for consideration (Federal Highway Administration 1997): one is to use the actual H-section area, and the other is to use the total rectangular section area. The actual degree of soil plugging involves many uncertainties and depends on a number of factors, such as the installation method and soil properties. For the purpose of clarity, no additional assumption of soil plug was introduced in handling the data at this stage. This issue is to be addressed separately in the future.

Conclusions

This paper describes the detailed results from a field study on instrumented steel H-piles jacked into dense sandy soils. The pile identified as PJ1 had an embedded length of 40.9 m and a design capacity of 3,540 kN, and the pile denoted by PJ2 had an embedment of 25.8 m and a design capacity of 2,950 kN. The performance of both piles was carefully monitored as the piles were jacked and load tested, and the effect of installation of adjacent piles was studied. The major observations may be summarized as follows:

1. Although both piles were founded on stiff sandy strata with extremely high SPT-N values, most of the applied loads were carried by shaft resistance rather than base resistance, implying that the design concept that piles in dense sandy soils have a very large base capacity and relatively small shaft loads might be inappropriate for jacked piles.
2. The effect of previous loading cycles on pile-soil stiffness and load distribution was insignificant. The creep settlement during the load test could be significantly reduced by the so-called "precreeping" effect attained in the termination of jacking.
3. Data from the second load test on PJ2, performed 34 days after the first load test, indicate that the end bearing increased by 25% with time. This finding is in agreement with reported observations on driven piles in sand.
4. The variation in pore pressures induced by jacking was associated with the progress of pile penetration. The pore pres-

sure measured by each piezometer increased as the pile tip approached and reached a maximum when the pile tip arrived at the piezometer level. As the pile tip passed, the pore pressure decreased. The rapid dissipation in pore pressure implies that it should not affect long-term pile behavior.

5. A nearby pile jacking produced large tensile stresses dominating in the major portion of an installed pile. Both the magnitude and distribution of the stresses were related to the penetration depth of the installing pile. The largest tensile stress took place at a location of approximately 1–2 m below the penetrating pile tip.

Acknowledgments

The financial support of the Research Grants Council of Hong Kong (HKU 7131/03E) and the University of Hong Kong is acknowledged. The assistance of Sunley Engineering and Construction Co., Ltd., and Gammon Skanska, Ltd., during the tests is also acknowledged.

References

- Been, K., and Jefferies, M. G. (1985). "A state parameter for sands." *Geotechnique*, 35(2), 99–112.
- Bolton, M. D. (1986). "The strength and dilatancy of sands." *Geotechnique*, 36(1), 65–78.
- Bond, A. J., and Jardine, R. J. (1995). "Effects of installing displacement piles in a high OCR clay." *Geotechnique*, 41(3), 341–363.
- Chow, F. C. (1995). "Field measurements of stress interactions between displacement piles in sand." *Ground Eng.*, 28(6), 36–40.
- Chow, F. C., Jardine, R. J., Nauroy, J. F., and Brucy, F. (1997). "Time-related increases in the shaft capacities of driven piles in sand." *Geotechnique*, 47(2), 353–361.
- Cooke, R. W., Price, G., and Tarr, K. (1979). "Jacked piles in London clay: A study of load transfer and settlement under working conditions." *Geotechnique*, 29(2), 113–147.
- Craig, W. H., and Sabagh, S. K. (1994). "Stress-level effects in model tests on piles." *Can. Geotech. J.* 31(1), 28–41.
- De Nicola, A., and Randolph, M. F. (1997). "The plugging behaviour of driven and jacked piles in sand." *Geotechnique*, 47(4), 841–856.
- Felenius, B. H. (2002). "Discussion of 'Side resistance in piles and drilled shafts,' by M. W. O'Neill." *J. Geotech. Geoenviron. Eng.*, 128(5), 446–448.
- Federal Highway Administration (FHWA). (1997). "Design and construction of driven pile foundations." *FHWA HI 97-013*, Washington, D.C.
- Guide to rock and soil descriptions* (1988). Geotechnical Control Office, Hong Kong.
- Hunt, C. E., Pestana, J. M., Bray, J. D., and Riemer, M. (2002). "Effect of pile driving on static and dynamic properties of soft clay." *J. Geotech. Geoenviron. Eng.*, 128(1), 13–24.
- Konrad, J. M., and Roy, M. (1987). "Bearing capacity of friction piles in marine clay." *Geotechnique*, 37(2), 163–175.
- Lehane, B. M., and Gavin, K. G. (2001). "Base resistance of jacked pipe piles in sand." *J. Geotech. Geoenviron. Eng.*, 127(6), 473–480.
- Lehane, B. M., Jardine, R. J., Bond, A. J., and Frank, R. (1993). "Mechanisms of shaft friction in sand from instrumented pile tests." *J. Geotech. Eng.*, 119(1), 19–35.
- Li, K. S., Ho, N. C. L., Tham, L. G., and Lee, P. K. K. (2003). *Case studies of jacked piling in Hong Kong*, Center for Research and Professional Development and University of Hong Kong, Hong Kong.
- Lumb, P. (1962). "The properties of decomposed granite." *Geotechnique*, 12(3), 226–243.

- Lumb, P., (1965). "The residual soils of Hong Kong." *Geotechnique*, 15(2), 180–194.
- Poulos, H. G. (1994). "Effect of pile driving on adjacent piles in clay." *Can. Geotech. J.*, 31(6), 856–867.
- Poulos, H. G., and Davis, E. H. (1980). *Pile foundation analysis and design*, Wiley, New York.
- Yang, J. (2005). "Discussion of 'Shaft resistance of single vertical and batter piles driven in sand,' by A. Hanna, and T. Nguyen." *J. Geotech. Geoenviron. Eng.* 131(1), 137–138.
- Yang, J., and Li, X. S., (2004). "State-dependent strength of sands from the perspective of unified modeling." *J. Geotech. Geoenviron. Eng.*, 130(2), 186–198.